JOURNAL OF BACTERIOLOGY, Mar. 2007, p. 1664–1674 Vol. 189, No. 5
0021-9193/07/$08.00+0 doi:10.1128/JB.01192-06

A Gene Cluster Involved in Degradation of Substituted Salicylates via *ortho* Cleavage in *Pseudomonas* sp. Strain MT1 Encodes Enzymes Specifically Adapted for Transformation of 4-Methylcatechol and 3-Methylmuconate[▽]

Beatriz Cámara, Piotr Bielecki, Filip Kaminski, Vitor Martins dos Santos, Iris Plumeier, Patricia Nikodem,† and Dietmar H. Pieper*

Division of Microbiology, HZI—Helmholtz Zentrum für Infektionsforschung, Inhoffenstrasse 7, D-38124 Braunschweig, Germany

Received 1 August 2006/Accepted 5 December 2006

***Pseudomonas* sp. strain MT1 has recently been reported to degrade 4- and 5-chlorosalicylate by a pathway assumed to consist of a patchwork of reactions comprising enzymes of the 3-oxoadipate pathway. Genes encoding the initial steps in the degradation of salicylate and substituted derivatives were now localized and sequenced. One of the gene clusters characterized (*sal*) showed a novel gene arrangement, with *salA*, encoding a salicylate 1-hydroxylase, being clustered with *salCD* genes, encoding muconate cycloisomerase and catechol 1,2-dioxygenase, respectively, and was expressed during growth on salicylate and chlorosalicylate. A second gene cluster (*cat*), exhibiting the typical *catRBCA* arrangement of genes of the catechol branch of the 3-oxoadipate pathway in *Pseudomonas* strains, was expressed during growth on salicylate. Despite their high sequence similarities with isoenzymes encoded by the *cat* gene cluster, the catechol 1,2-dioxygenase and muconate cycloisomerase encoded by the *sal* cluster showed unusual kinetic properties. Enzymes were adapted for turnover of 4-chlorocatechol and 3-chloromuconate; however, 4-methylcatechol and 3-methylmuconate were identified as the preferred substrates. Investigation of the substrate spectrum identified 4- and 5-methylsalicylate as growth substrates, which were effectively converted by enzymes of the *sal* cluster into 4-methylmuconolactone, followed by isomerization to 3-methylmuconolactone. The function of the *sal* gene cluster is therefore to channel both chlorosubstituted and methylsubstituted salicylates into a catechol *ortho* cleavage pathway, followed by dismantling of the formed substituted muconolactones through specific pathways.**

Aerobic degradation of aromatic compounds usually involves their successive activation and modification such that they are channeled toward a few dihydroxylated intermediates (17, 38). Catechol is the common intermediate during the degradation of a significant number of aromatic compounds such as benzoate, benzene, phenol, or salicylate and can be subject to either intradiol cleavage by a catechol 1,2-dioxygenase (C12O) or extradiol cleavage by a catechol 2,3-dioxygenase (17, 38). Enzymes for catechol degradation via intradiol cleavage are encoded by the catechol branch of the 3-oxoadipate pathway (15). *Pseudomonas* strains usually contain a *catRBCA* gene cluster (16, 33, 54) comprising genes encoding catechol 1,2-dioxygenase (CatA), muconate cycloisomerase (MCI; CatB), and muconolactone isomerase (CatC), which are controlled by a LysR type regulator (CatR) in response to the inducer muconate (17). However, various permutations with respect to enzyme distribution, regulation, and gene organization have also been observed (15, 30, 47, 55). The proteobacterial pathway for catechol degradation is not suited for the degradation of chlorosubstituted or methylsubstituted catechols. Methylcatechols, when channeled into the intradiol pathway, are transformed into methylsubstituted muconolactones as dead-end products (8, 25). Enzymes involved in 4-methylmuconolactone degradation have thus far been characterized only from *Rhodococcus rhodochrous* N75 and *Cupriavidus necator* JMP134 and comprise a 4-methylmuconolactone 4-methylisomerase, forming 3-methylmuconolactone, as a key enzyme (7, 13, 43). Bacteria capable of degrading chloroaromatics via chlorocatechols usually contain enzymes of the chlorocatechol pathway (48, 49), involving *ortho* cleavage by a chlorocatechol 1,2-dioxygenase with high activity against chlorocatechols (11), a chloromuconate cycloisomerase with high activity against chloromuconates (53), a dienelactone hydrolase active against both *cis*- and *trans*-dienelactone (4-carboxymethylenebut-2-en-4-olide) (53), and a maleylacetate reductase (23). In phylogenetic analyses, chlorocatechol and catechol 1,2-dioxygenases constitute different subfamilies of the family of intradiol dioxygenases. Chlorocatechol 1,2-dioxygenases are of broad substrate specificity, whereas catechol 1,2-dioxygenases exhibit relatively low activity with 4-chlorocatechol and negligible activity with 3-chlorocatechol (38). More importantly, muconate and chloromuconate cycloisomerases differ not only in substrate specificity but also in the reaction performed. Chloromuconate cycloisomerases catalyze a dehalogenation of 3-chloromuconate to form *cis*-dienelactone (53), and muconate cycloisomerases catalyze the formation of protoanemonin (1) with 4-chloromuconolactone as a reaction intermediate (1, 32). 2-Chloromuconate is dehalogenated only by chloromuconate cycloisomerases (59), while mu-

* Corresponding author. Mailing address: Bereich Mikrobiologie, AG Biodegradation, HZI—Helmholtz Zentrum für Infektionsforschung, Inhoffenstrasse 7, D-38124 Braunschweig, Germany. Phone: 49 531 6181 4200. Fax: 49 531 6181 4499. E-mail: dpi@helmholtz-hzi.de.

† Present address: Novo Nordisk A/S, Hallas Allé, DK-4400 Kalundborg, Denmark.

▽ Published ahead of print on 15 December 2006.

conate cycloisomerases form 2-chloro- and 5-chloromuconolactone (60).

Pseudomonas sp. strain MT1 has been reported to degrade 4- and 5-chlorosalicylate by a different metabolic route (32). The substrates are transformed by a salicylate 1-hydroxylase into 4-chlorocatechol, which is subject to ring cleavage by catechol 1,2-dioxygenase to yield 3-chloromuconate. It is suggested that *trans*-dienelactone hydrolase acts on 4-chloromuconolactone as an intermediate in the muconate cycloisomerase-catalyzed transformation of 3-chloromuconate, thus preventing protoanemonin formation in favor of maleylacetate (32). Maleylacetate is reduced to 3-oxoadipate by maleylacetate reductase. Chlorocatechol degradation in strain MT1 was thus assumed to occur by a pathway consisting of a patchwork of reactions known from the 3-oxoadipate pathway (catechol 1,2-dioxygenase, muconate cycloisomerase), the chlorocatechol pathway (maleylacetate reductase), and a *trans*-dienelactone hydrolase. However, the kinetic parameters of the characterized muconate cycloisomerase (that is, its preference for 3-chloromuconate over muconate as a substrate) set it apart from previously characterized muconate cycloisomerases (32, 53, 58). Moreover, salicylate degradation via catechol is usually performed via *meta* cleavage, and an operon structure comprising genes encoding a LysR type regulator (NahR), a salicylate 1-hydroxylase (NahG), a catechol 2,3-dioxygenase (NahH), and subsequent enzymes of the *meta* cleavage pathway is usually conserved (2, 9, 63). However, no extradiol dioxygenase activity was observed in either salicylate-grown or chlorosalicylate-grown cells of MT1 (32), suggesting that the gene encoding salicylate 1-hydroxylase is not clustered with the *meta* cleavage pathway.

In the current report we analyzed the genetic organization and expression of two catabolic gene clusters of MT1. Detailed characterization of the kinetic parameters of the enzymes encoded revealed that one of the clusters was specifically adapted for channeling substituted salicylates into the catechol *ortho* cleavage pathway.

MATERIALS AND METHODS

Bacterial strains. *Pseudomonas* sp. strain MT1 was grown and cell extracts prepared as previously described (32).

Enzyme assays. Salicylate hydroxylase (SalOH), C12O, catechol 2,3-dioxygenase, and MCI were measured spectrophotometrically as described previously (3, 11, 53, 61). 4-Methylmuconolactone 4-methylisomerase activity was determined by high-performance liquid chromatography (HPLC) following its transformation into 3-methylmuconolactone (43). The activities of muconate cycloisomerases MCI_{catB} and MCI_{salC} with 2-chloromuconate (100 μM) and 3-chloromuconate were determined by HPLC. As much as 1 U/ml of purified enzymes was used for determining 2-chloromuconate transformation, whereas 3-chloromuconate transformation was determined using 5 to 30 mU/ml (MCI_{catB}) or 0.2 to 1 mU/ml (MCI_{salC}) (units were measured with 0.1 mM muconate as a substrate).

Specific activities (units per gram of protein) are expressed as micromoles of substrate converted or product formed per minute per gram of protein at 25°C. Protein concentrations were determined by the Bradford procedure using the Bio-Rad protein assay with bovine serum albumin as a protein standard (4).

Analysis of kinetic data. V_{max}, k_{cat}, and apparent K_m values of C12O's with catechols were determined using 1 to 100 μM substrate in air-saturated buffer, and kinetic data were calculated from the initial velocities using the Michaelis-Menten equation by nonlinear regression (KaleidaGraph; Synergy Software). Since very low K_m values were indicated by this method, kinetic data were finally determined from progress curves obtained from reactions with initial substrate concentrations of 10 μM, as previously described for determination of low K_m values of catechol 2,3-dioxygenases (20). The data sets obtained were fit to the Michaelis-Menten equation by nonlinear regression (KaleidaGraph; Synergy Software).

V_{max}, k_{cat}, and apparent K_m values of SalOH with NADH were determined using 2 to 100 μM NADH and 200 μM salicylate in air-saturated buffer, and those with differently substituted salicylates were determined using 200 μM NADH and 1 to 100 μM substrate. Rate constants of SalOH with 5-chlorosalicylate were also determined from progress curves obtained from reactions with initial substrate concentrations of 10 μM. The kinetic parameters of MCI_{catB} and MCI_{salC} with muconate, 2-methylmuconate, and 3-methylmuconate were determined using 5 to 100 μM substrate. Transformation of 3-chloromuconate was determined by HPLC analysis at substrate concentrations of 50 μM to 500 μM. Samples were taken during the reaction time, and protoanemonin formation was directly analyzed by HPLC analysis. At least two independent experiments were performed for each value. K_m and V_{max} values were calculated by nonlinear regression to the Michaelis-Menten equation by using KaleidaGraph (Synergy Software). Turnover numbers (k_{cat} values) were calculated assuming subunit molecular masses of 34,209 ($C12O_{catA}$), 34,233 ($C12O_{salD}$), 41,076 (MCI_{catB}), 40,248 (MCI_{salC}), and 50,712 (SalOH) Da, respectively.

Enzyme separation and purification. SalOH, catechol 1,2-dioxygenases ($C12O_{catA}$ and $C12O_{salD}$), and muconate cycloisomerases (MCI_{catB} and MCI_{salC}) were purified from cell extracts of salicylate-, 4-methylsalicylate-, or 5-chlorosalicylate-grown cells using a fast protein liquid chromatography system (Amersham Biosciences). All protein elutions were performed in Tris-HCl (50 mM, pH 7.5, 2 mM $MnCl_2$).

For analyzing the presence and abundance of $C12O_{catA}$, $C12O_{salD}$, MCI_{catB}, and MCI_{salC} under different growth conditions, cell extracts (10 to 25 mg of protein) were mixed with 4 M $(NH_4)_2SO_4$ to give a final concentration of 1 M $(NH_4)_2SO_4$ and were applied to a SOURCE 15PHE PE 4.6/100 (hydrophobic interaction) column (Amersham Pharmacia Biotech). Proteins were eluted by a linear gradient of $(NH_4)_2SO_4$ (1 M to 0 M) over 25 ml with a flow of 0.25 ml/min. Fraction volumes were 0.5 ml. Hydrophobic interaction chromatography (HIC) separated $C12O_{catA}$ (0.16 ± 0.04 M) and $C12O_{salD}$ (0.45 ± 0.04 M) and partially separated MCI_{catB} (0.12 ± 0.06 M), and MCI_{salC} (0.06 ± 0.06 M). Since HIC was not suitable for SalOH detection, the presence and abundance of SalOH were analyzed by separation through anion-exchange chromatography using a MonoQ HR 5/5 column (Amersham Pharmacia Biotech). Cell extracts were directly applied and proteins eluted by a linear gradient of 0 to 0.5 M NaCl over 25 ml with a flow of 0.2 ml/min. SalOH eluted at 0.17 ± 0.02 M NaCl. $C12O_{catA}$ and $C12O_{salD}$ coeluted at 0.28 ± 0.02 M NaCl, and MCI_{catB} and MCI_{salC} coeluted at 0.24 ± 0.02 M NaCl.

For purification of $C12O_{catA}$ and $C12O_{salD}$, 40 mg of protein from salicylate-grown cells was applied to a MonoQ HR 5/5 column and the proteins eluted as described above. Fractions containing C12O activity were combined, concentrated by Centricon YM-50 (Millipore) to a final volume of 1 ml, and supplemented with 2 M $(NH_4)_2SO_4$ to give a final concentration of 1 M $(NH_4)_2SO_4$. Subsequent HIC, as described above, resulted in separation of $C12O_{catA}$ and $C12O_{salD}$.

For purification of SalOH and MCI_{catB}, two 40-mg aliquots of protein from salicylate-grown cells were applied to a MonoQ HR 5/5 column and the proteins eluted as described above. Fractions containing muconate cycloisomerizing or salicylate hydroxylase activities were pooled separately and concentrated to final volumes of 1 and 0.2 ml, respectively. The muconate cycloisomerase-containing protein solution was supplemented with 2 M $(NH_4)_2SO_4$ to give a final concentration of 1 M $(NH_4)_2SO_4$ and was separated by HIC, as described above. Fractions eluting at 0.12 ± 0.04 M and exhibiting high activity against muconate but low activity against 3-methylmuconate (MCI_{catB}) were pooled, whereas fractions eluting at 0.06 ± 0.06 M and exhibiting relatively high activity against 3-methylmuconate (MCI_{salC}) were discarded. The pooled fractions were further concentrated by ultracentrifugation and separated by HIC using a linear gradient of $(NH_4)_2SO_4$ (0.5 M to 0 M) over 17 ml with a flow rate of 0.25 ml/min. Fractions with high activity against muconate but low activity against 3-methylmuconate eluted at 0.14 ± 0.06 M $(NH_4)_2SO_4$ and were pooled. Fractions eluting at <0.14 ± 0.06 M $(NH_4)_2SO_4$ were discarded, since they may contain minor amounts of contaminating MCI_{salC}.

SalOH was further purified by gel filtration using a Superose 12 HR10/10 column (Amersham Pharmacia Biotech) with 20 ml Tris-HCl (50 mM, 100 mM NaCl, pH 7.5) as an eluent with a flow rate of 0.3 ml/min. Two fractions (0.5 ml each) exhibiting high activity with salicylate were pooled.

MCI_{salC} was purified from 5-chlorosalicylate-grown cells as previously described (32).

Electrophoretic methods. Sodium dodecyl sulfate-polyacrylamide gel electrophoresis (SDS-PAGE) was performed on a Bio-Rad Miniprotein II apparatus as previously described (26), with acrylamide concentrations of 5 and 10% (wt/vol) used for the concentrating and separating gels, respectively. The proteins were

stained with Coomassie brilliant blue (Serva). A PageRuler protein ladder (Fermentas) was used as a marker.

Quantification of proteins in partially purified fractions. For quantification of C12O proteins, MCI_{catB}, and SalOH in partially purified fractions, 0.3 to 15 μg of protein was separated by SDS-PAGE. Gels were stained with Ruthenium II tris (bathophenantroline disulfonate) as previously described (20) and scanned using a Fujifilm LAS-1000 charge-coupled device camera. The fluorescence intensity was integrated, and the relative intensities of the bands corresponding to $C12O_{catA}$, $C12O_{salD}$, MCI_{catB}, and SalOH were determined using the AIDA 2.1 software package (Raytest Isotopenmessgeräte GmbH).

Amino acid sequencing. N-terminal amino acid sequences were determined as previously described (19).

DNA isolation and preparation of genome libraries. Genomic DNA of *Pseudomonas* sp. strain MT1 was isolated with the G NOME DNA kit (BIO 101 Systems). A fosmid library was prepared in pCC1FOS according to the manufacturer's recommendations (Epicentre). Genomic DNA was randomly sheared by pipetting to give approximately 40-kb fragments for ligation into pCC1FOS. Ligated DNA was packaged with MaxPlax Lambda packaging extracts, transduced into *Escherichia coli* strain EPI300-T1, and spread onto LB agar plates containing 12.5 μg/ml chloramphenicol. A total of 282 individual clones were analyzed.

For preparation of the phage library, DNA was partially digested with Sau3AI and size fractionated by ultracentrifugation in a sucrose gradient (51). After overnight precipitation with polyethylene glycol 6000, the recovered fraction of 4- to 12-kbp DNA fragments was ligated into the BamHI/calf intestine alkaline phosphatase-treated ZAP Express vector (Stratagene). Gigapack III gold packaging extract (Stratagene) was used for packaging the ligated DNA into functional phage particles.

Identification of the *cat* gene cluster of strain MT1. Part of the *catA* gene encoding $C12O_{catA}$ was amplified by two rounds of PCR (annealing temperature, 50°C) using primers C12OA-F2 (TGCCGAAGTYCARAAYTTTC) and C12OA-R2 (TTGATCTGSGTGGTCAG), which were designed based on the N-terminal protein sequence and on an alignment of the C12O DNA sequences from *Pseudomonas* strains, respectively. The fragment generated (approximately 700 bp) was cloned into pGEM-T Easy (Promega), transformed into *E. coli* XL10-Gold (Stratagene), and sequenced. The fosmid library was screened by PCR (annealing temperature, 59°C) using primers specific for *catA* (incoA F, CTATCGCATCCTGCGTGACT; incoA R, CCGGGTCGAAGTACGAGT AG). A positive fosmid clone was purified with the FosmidMAX DNA purification kit (Epicentre), and the complete *catA* sequence was obtained by direct sequencing from the fosmid. Sequence information upstream of the *catA* gene was obtained by PCR using MT1 genomic DNA, primer coA R1 (GCGAGGT CTTCGATGATGTT) (annealing at positions 127 to 146 of *catA*), and the degenerate primer Areg R2 (TCDATCATNCKWAGRCAATG) (presumed to anneal to *catR* in a putative *catRBCA* operon). The fragment (approximately 2.6 kb) obtained after two rounds of PCR using an annealing temperature of 52.5°C was ligated into the pGEM-T Easy vector (Promega), subsequently cloned into *E. coli* XL10-Gold cells (Stratagene), and verified by sequencing to comprise part of *catR*, the complete *catBC* genes, and part of *catA*.

Identification of the *sal* gene cluster. Part of the *salC* gene, encoding MCI_{salC}, was amplified by PCR (annealing temperature, 45°C) using primers MCI_F1 (CTIGAYGCCIARGGCAARCG) and MCI_R (CRTCCCAITAYTGRTTIAC GTC), which were designed based on conserved muconate cycloisomerase protein sequences (LDAQGKR and DVNQYWD, respectively). The 279-bp fragment generated was subsequently cloned into the TOPO vector (Invitrogen), identified by sequencing as probably encoding part of a muconate cycloisomerase, and used as a template to generate a dioxigenin-labeled probe by applying the PCR DIG labeling mix (Roche).

The phage library was plated onto NZY agar (up to 15 plaques/cm^2). After overnight growth at 37°C, plaques were lifted onto a nylon membrane (Hybond N+; Amersham Biosciences), which was then denatured (with 1.5 M NaCl–0.5 M NaOH for 2 min), neutralized (with 1.5 M NaCl–0.5 M Tris [pH 8.0] for 5 min), and rinsed (with 2× SSC [1× SSC is 0.15 M NaCl plus 0.015 M sodium citrate]–0.2 M Tris [pH 7.5] for 30 s). Blotted DNA was cross-linked to the membrane with UV light. The DNA probe was hybridized to the membrane overnight at 68°C in hybridization buffer (5× SSC, 2% [wt/vol] blocking reagent, 0.1% [wt/vol] *N*-sodium lauryl sarcosine, and 0.02% [wt/vol] SDS) with further stringent washing steps and a detection procedure as recommended for dioxigenin labeling by the manufacturer (Roche). Hybridization was repeated for selected phages to ensure error-free plaque assignment and single-clone representation.

Phages were converted into phagemids in the host cells after coinfection with ExAssist helper phage (Stratagene). Excised phagemids were cloned into XLOLR cells in LB medium with kanamycin (50 μg/ml). Phagemid DNA was isolated with a NucleoSpin plasmid minikit (Macherey-Nagel). Inserts from three selected clones (3,953 bp, 6,394 bp, and 9,327 bp) were sequenced with custom primers.

DNA sequencing and sequence analysis. PCR products were purified with the QIAquick PCR purification kit and were sequenced using the ABI PRISM BigDye Terminator (version 1.1) ready reaction cycle sequencing kit (Applied Biosystems) and an ABI PRISM 3100 genetic analyzer (Applied Biosystems). Raw sequence data from both strands were assembled with Sequencher software, version 4.0.5 (Gene Codes Corporation). DNA and protein similarity searches were performed using the BLASTN and BLASTP programs from the NCBI website. Alignments were generated with the CLUSTALX 1.8 windows interface of the CLUSTALW program using default values (56). Phylogenetic trees were constructed using the neighbor-joining algorithm of the CLUSTAL program. Distances were generated using the Kimura matrix, and tree stability was supported through bootstrap analysis (100 replicates). Trees were visualized with TREEVIEW 1.6.6 (34).

Gene expression studies. *Pseudomonas* sp. strain MT1 cells were harvested during exponential growth with acetate (8 mM; growth rate, 0.24 h^{-1}), salicylate (2 mM), or 5-chlorosalicylate (2 mM). Samples (7 ml; optical density at 600 nm, 0.15) were immediately transferred to a tube containing 7 ml of RNAprotect (QIAGEN), vortexed, and centrifuged at 2,500 × *g* for 20 min. RNA was isolated by using a QIAGEN RNeasy minikit. RNA was quantified photometrically at 260 nm, and its integrity was evaluated by electrophoresis in 1.2% agarose. Reverse transcription and quantitative real-time PCR were performed using a QuantiTect SYBR green reverse transcription-PCR (RT-PCR) kit (QIAGEN) for one-step RT-PCR in a Rotor-Gene 2000 real-time PCR machine (Corbett Research). Transcripts of *salA*, *salC*, *catA*, and *catB* were quantified with the following primer pairs: SalA-F (CGCGCCAAGGGCATCAATACTC), SalA-R (GCTGG AGCGGTCGGAAAGGAAC), SalC-F (CACACCATTTCGCAGCAGACC), SalC-R (ACTGGCGTCCATACCGATCAAG), CatA-F (TCAAAATTTCCCA CACTGCTGA), CatA-R (TGACCGCTTTCCAGAACTCTTC), CatB-F (CCT GAAGATTGCCAAGAGTGGT), and CatB-R (AGTTTGTTCAGGGTGACG AAGG). To correct for differences in the amount of starting material, the ribosomal *rpsL* gene was chosen as a housekeeping reference gene. The PCR primers used for quantifying *rpsL* transcripts were rpsL-F (GCAAGCGAATG GTCGACAAGA) and rpsL-R (CGCTGTGCTCTTGCAGGTTGTGA) (12). Real-time PCRs were carried out in 20-μl reaction mixtures containing 50 ng of RNA. The thermal cycling conditions were as follows: 30 min at 50°C for reverse transcription; 15 min at 95°C for initial activation of HotStarTaq DNA polymerase, followed by 40 cycles of 15 s at 94°C, 30 s at 62°C, and 30 s at 72°C. Data collection was performed during each extension phase. Melt curve analysis and gel electrophoresis showed high specificity of primers and negligible formation of primer-dimers during amplification (data not shown). The relative expression ratios are presented as changes in the ratio of gene expression between the target gene and the reference gene (*rpsL*) compared to noninducing conditions (for acetate-grown cells, this ratio was set at 1). The expression ratios were calculated using REST-RG beta software (37), with crossing points and amplification efficiencies for each sample obtained from Rotor-Gene 2000 software, version 4.6 (Corbett Research), and were tested for significance by a pairwise fixed reallocation randomization test implemented in REST-RG.

Analytical methods. HPLC was performed with a Lichrospher SC 100 RP8 reversed-phase column (125 by 4.6 mm; Bischoff). Methanol-H_2O containing 0.1% (vol/vol) H_3PO_4 was used as the eluant at a flow rate of 1 ml/min. The column effluent was monitored simultaneously at 210, 260, and 280 nm by a diode array detector (Shimadzu). Typical retention volumes using 18% (vol/vol) methanol were as follows: 2-chloro-*cis*,*cis*-muconate, 10.5 ml; 3-chloro-*cis*,*cis*-muconate, 9.6 ml; *cis*-dienelactone, 5.2 ml; protoanemonin, 4.9 ml; 4-methylmuconolactone, 1.4 ml; 3-methylmuconolactone, 1.2 ml.

Chemicals. 3-Chloro- and 4-chlorocatechol were obtained from Helix Biotech. 2-Methyl-, 3-methyl-, and 3-chloro-*cis*,*cis*-muconate were freshly prepared from 3-methyl-, 4-methyl-, and 4-chlorocatechol, respectively, in Tris-HCl (50 mM, pH 7.5, 2 mM $MnCl_2$) using chlorocatechol 1,2-dioxygenase TetC of *Pseudomonas chlororaphis* RW71 (44) or partially purified $C12O_{salD}$ free of muconate cycloisomerizing activity. *cis*-Dienelactone was kindly provided by Walter Reineke (Bergische Universität—Gesamthochschule Wuppertal, Wuppertal, Germany) and Stefan Kaschabeck (TU Bergakademie Freiberg, Freiberg, Germany). Protoanemonin, 4-methylmuconolactone, 3-methylmuconolactone, (+)-muconolactone, *cis*,*cis*-muconate, and 2-chloro-*cis*,*cis*-muconate were prepared as described previously (1, 39, 42, 46).

Nucleotide sequence accession number. The nucleotide sequences reported in this study have been deposited in the DDBJ/EMBL/GenBank databases under accession numbers DQ870624 (*cat* gene cluster) and AY944685 (*sal* gene cluster).

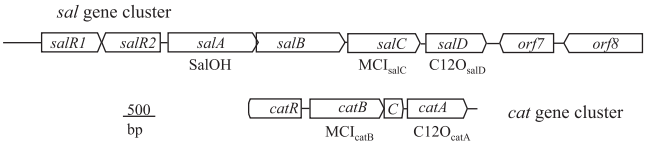

FIG. 1. Gene organization of a 9,886-bp and a 3,554-bp region from *Pseudomonas* sp. strain MT1 containing the *sal* and *cat* gene clusters. Arrows indicate gene orientations. *salA*, salicylate 1-hydroxylase gene; *salD* and *catA*, catechol 1,2-dioxygenase genes; *salC* and *catB*, muconate cycloisomerase genes; *catC*, muconolactone isomerase gene; *salB*, putative transporter gene; *salR1*, *salR2*, and *catR*, putative regulator genes. The *catR* gene was only partially sequenced. Abbreviations of encoded enzymes are given below the gene clusters.

RESULTS

Genetic analysis of the *sal* gene cluster. A muconate cycloisomerase, which was characterized by its substrate preference of 3-chloromuconate over muconate, has previously been identified in *Pseudomonas* sp. strain MT1 (32). Since this enzyme was assumed to be important for both salicylate and chlorosalicylate degradation by this strain, analysis of the encoding gene region was performed. Inspection of the 9,886-bp sequenced region (Fig. 1) identified eight complete open reading frames (ORFs) and one partial ORF. ORF5, designated *salC*, encoded an enzyme with a deduced N-terminal sequence identical to that of the previously characterized muconate cycloisomerase (32). Phylogenetic analysis of the deduced protein (further termed MCI$_{salC}$) revealed high sequence homology with proteobacterial muconate cycloisomerases, specifically those of *Pseudomonas* strains (Fig. 2A). The deduced product of the downstream *salD* gene showed high sequence homology sequence with proteobacterial catechol 1,2-dioxygenases (Fig. 2B). However, a gene encoding a muconolactone isomerase (usually clustered in *Pseudomonas* strains with genes encoding muconate cycloisomerases and catechol 1,2-dioxygenases (16, 17) could not be localized in the sequenced region. In contrast, *salC* was preceded by ORFs with high homology to genes encoding salicylate 1-hydroxylases (*salA*) and permeases of the major facilitator subfamily (*salB*). The *salA* gene product showed the highest similarity to *nahG* gene products, single-component flavoprotein monooxygenases responsible for transforming salicylate produced from naphthalene into catechol (Fig. 2C), and the *salB* gene product showed the highest similarity to *benK* (benzoate transporters) transporters of the major facilitator superfamily (64% identity of the deduced amino acid sequence to the *benK* gene product of *Pseudomonas* sp. strain ND6 [28]). Transcribed divergently toward *salA*, an ORF putatively encoding a regulatory protein of the LysR family was identified and termed *salR2* (Fig. 1). Phylogenetic analysis revealed that the putative gene product clustered with *nahR* gene products (Fig. 2D), which are usually responsive to salicylate (14). Transcribed convergently toward *salR2*, a second gene (*salR1*), putatively encoding a LysR type regulator, was observed and showed homology to NahR regulators. Transcribed convergently toward *salD*, a putative gene (*orf7*) encoding a 2-hydroxymuconic semialdehyde hydrolase (60% amino acid identity to TdnF of *Pseudomonas putida* UCC22 [D85415]) was preceded by an incomplete ORF (*orf8*) of a putative transporter of the resistance-nodulation-cell division family (56% amino acid identity to the putative transporter PP3302 of *P. putida* KT2440 [NC_002947]).

Two catechol 1,2-dioxygenases in *Pseudomonas* sp. strain MT1. Since *Pseudomonas* strains usually contain a *catRBCA* cluster (17), which also encodes muconate cycloisomerase (*catB*) and catechol 1,2-dioxygenase (*catA*), we analyzed if different catechol-transforming activities were induced during growth on salicylate. Two distinct catechol 1,2-dioxygenase activities, eluting, respectively, at 0.45 ± 0.04 M $(NH_4)_2SO_4$ and 0.16 ± 0.04 M $(NH_4)_2SO_4$, were observed when cell extracts of salicylate-grown MT1 cells were subjected to HIC. The respective fractions were analyzed by SDS-PAGE, and prominent bands of 33 ± 2 kDa were subjected to N-terminal sequencing. The N terminus of the protein eluting at 0.45 ± 0.04 M $(NH_4)_2SO_4$ (TVKISHTAEVQDLIK) was identical to that of the predicted *salD* gene product and is termed C12O$_{salD}$. The N terminus of the protein eluting at 0.16 ± 0.04 M $(NH_4)_2SO_4$ (MNVKISHTAEVQNFL) (termed C12O$_{catA}$) showed high similarity to that of catechol 1,2-dioxygenase of *Pseudomonas putida* KT2440 (accession number NC_002947). In contrast to that in salicylate-grown cells, C12O$_{catA}$ activity was absent in 5-chlorosalicylate-grown cells, as was apparent by the absence of activity in fractions eluting at 0.16 ± 0.04 M $(NH_4)_2SO_4$ after HIC.

To analyze if C12O$_{salD}$, like MCI$_{salC}$, has properties differing from those of typical proteobacterial enzymes of the 3-oxoadipate pathway, kinetic data were measured for fractions obtained after subsequent anion exchange and HIC of salicylate-grown cell extracts (Table 1). k_{cat} values of 8.7 ± 1.4 s^{-1} (C12O$_{catA}$) and 7.5 ± 0.8 s^{-1} (C12O$_{salD}$) were obtained for catechol; these are in the same order of magnitude as those reported for catechol 1,2-dioxygenases from other proteobacteria (24, 31, 52). Like previously characterized proteobacterial catechol 1,2-dioxygenases, both enzymes showed negligible activity with 3-chlorocatechol (5, 10). However, the enzymes differed in their turnover rates for 4-chlorocatechol and especially for 4-methylcatechol, where C12O$_{salD}$ exhibited significantly higher rates (Table 1). Both enzymes also differed with respect to their apparent K_m values. Like other proteobacterial dioxygenases (10, 24, 52), C12O$_{catA}$ showed the highest apparent K_m with 4-methylcatechol. This contrasts with C12O$_{salD}$, which showed relatively low affinity for catechol and 3-methylcatechol (Table 1). The k_{cat}/K_m specificity constants indicate that catechol is the preferred substrate for C12O$_{catA}$ whereas 4-methylcatechol is the preferred substrate for C12O$_{salD}$. Thus, C12O$_{salD}$ shows a substrate specificity profile clearly different from those of previously described C12O's.

Identification of a *cat* gene cluster in *Pseudomonas* sp. strain MT1. To analyze if C12O$_{catA}$ is encoded by a typical *Pseudomonas catRBCA* gene cluster, sequence information (totaling 3,554 bp) was obtained as outlined in Materials and Methods. Analysis of this region revealed three complete ORFs and one partial ORF (Fig. 1). *catA* encoded a catechol 1,2-dioxygenase with a deduced N-terminal sequence identical to that identified above for C12O$_{catA}$. Upstream of *catA*, two ORFs with high sequence similarity to genes encoding muconolactone isomerase (*catC*, with 95% identity of the deduced amino acid sequence to the *catC* gene product of an uncultured bacterium [AB186499] and 86% identity to the *catC* gene product of *Pseudomonas fluorescens* Pf-5 [NC_004129]) and genes encod-

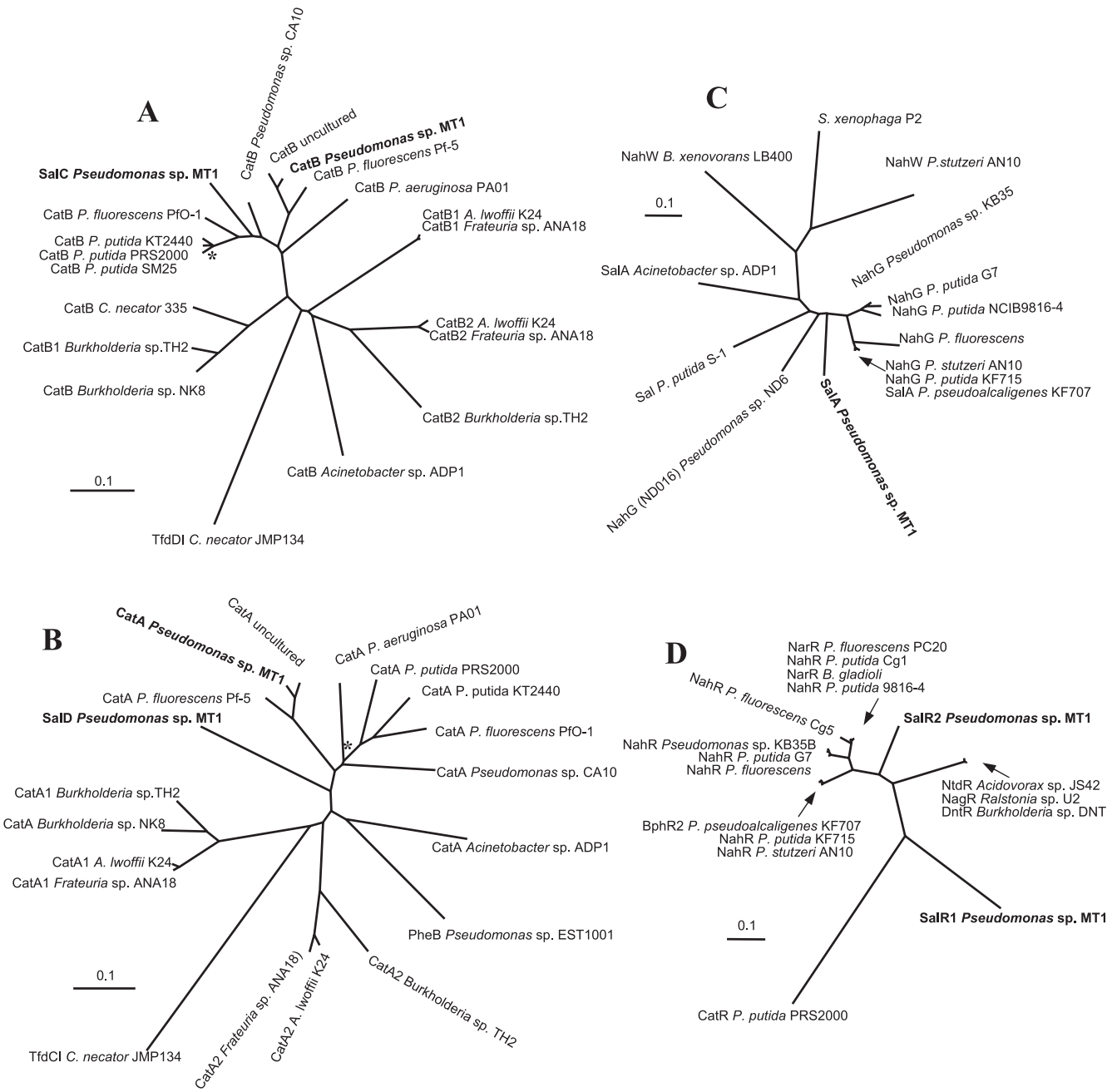

FIG. 2. Dendrograms showing the relatedness of muconate cycloisomerases (A), catechol 1,2-dioxygenases (B), salicylate 1-hydroxylases (C), and LysR family regulators similar to NahR (D). The dendrograms were calculated using Treeview 1.6.6 based on sequence alignments calculated by ClustalX 1.81 using the default options. Sequences of deduced proteins of the *sal* and *cat* gene clusters of *Pseudomonas* sp. strain MT1 are boldfaced. Bars correspond to an estimated evolutionary distance of 0.1 amino acid substitution per site. Asterisks indicate bootstrap values of <50%. The chloromuconate cycloisomerase TfdDI (A) and the chlorocatechol 1,2-dioxygenase TfdCI (B) of *C. necator* JMP134 and the CatR LysR type regulator (D) of *P. putida* PRS2000 are included as outgroups. Accession numbers are as follows: for *Burkholderia* sp. strain NK8 CatB, AB024746; for *Burkholderia* sp. strain TH2 CatB1, AB035488; for *C. necator* 335 CatB, AF042281; for *P. putida* SM25 CatB, AY028997; for *P. putida* PRS2000 CatB, P08310; for *P. putida* KT2440 CatB, NC_002947; for *P. fluorescens* PFO-1 CatB, NC_007492; for *Pseudomonas* sp. strain CA10 CatB, AB047272; for uncultured bacterium CatB, AB186499; for *P. fluorescens* Pf-5 CatB, NC_004129; for *P. aeruginosa* PA01 CatB, NC_002516; for *Acinetobacter lwoffii* CatB1, O33946; for *Frateuria* sp. strain ANA18 CatB1, AB009343; for *A. lwoffii* K24 CatB2, O33949; for *Frateuria* sp. strain ANA18 CatB2, T48870; for *Burkholderia* sp. strain TH2 CatB2, AB035325; for *Acinetobacter* sp. strain ADP1 CatB, Q43931; for *C. necator* JMP134 TfdDI, P05404; for *Frateuria* sp. strain ANA18 CatA1, AB009343; for *A. lwoffii* K24 CatA1, O33948; for *Burkholderia* sp. strain NK8 CatA, AB024746; for *Burkholderia* sp. strain TH2 CatA1, AB035483; for *P. fluorescens* Pf-5 CatA, CP00076; for uncultured bacterium CatA, AB186499; for *P. aeruginosa* PA01 CatA, NC_002516; for *P. putida* PRS2000 CatA, U12557; for *P. putida* KT2440 CatA, NC_002947; for *P. fluorescens* PfO-1 CatA, CP000094; for *Pseudomonas* sp. strain CA10 CatA, AB047272; for *Acinetobacter* sp. strain ADP1 CatA, P07773; for *Pseudomonas* sp. strain EST1001 PheB, P31019; for *Burkholderia* sp. strain TH2 CatA2, AB03525; for *A. lwoffii* K24 CatA2, O33950; for *Frateuria* sp. strain ANA18 CatA2, AB009373; for *C. necator* JMP134 TfdCI, P05403; for *P. stutzeri* AN10 NahR, AF039534; for *P. putida* KF715 NahR, AY294313; for *Pseudomonas pseudoalcaligenes* KF707 BphR2, DQ100350; for *P. fluorescens* NahR, AF491315; for *P. putida* G7 NahR, P10183; for

TABLE 1. Substrate specificities of catechol 1,2-dioxygenases $C12O_{catA}$ and $C12O_{salD}$ from *Pseudomonas* sp. strain MT1[a]

Enzyme and substrate	Activity with 0.1 mM substrate (U/mg C12O)	K_m (μM)	k_{cat} (s^{-1})	k_{cat}/K_m (s^{-1} μM^{-1})
$C12O_{catA}$				
Catechol	15.3 ± 2.5	0.8 ± 0.2	8.7 ± 1.4	10.9
4-Chlorocatechol	1.2 ± 0.2	1.0 ± 0.4	0.7 ± 0.1	0.7
3-Chlorocatechol	0.05 ± 0.015	ND[b]	ND	ND
4-Methylcatechol	4.4 ± 0.5	9.9 ± 2.7	2.7 ± 0.3	0.3
3-Methylcatechol	1.4 ± 0.4	1.0 ± 0.2	0.8 ± 0.2	0.8
$C12O_{salD}$				
Catechol	12.3 ± 1.4	7.5 ± 0.9	7.5 ± 0.8	1
4-Chlorocatechol	2.9 ± 0.4	1.0 ± 0.3	1.7 ± 0.2	1.7
3-Chlorocatechol	0.03 ± 0.005	ND	ND	ND
4-Methylcatechol	35.8 ± 2.1	1.7 ± 0.6	20.7 ± 1.2	12.2
3-Methylcatechol	3.8 ± 0.5	5.6 ± 0.8	2.3 ± 0.3	0.4

[a] The kinetic constants were determined as described in Materials and Methods using samples where the target protein comprised 41% ± 2% ($C12O_{catA}$) or 57% ± 3% ($C12O_{salD}$) of the total protein content. Activities were calculated based on the amount of target protein applied and on subunit molecular masses of 34.233 kDa for $C12O_{salD}$ and 34.209 kDa for $C12O_{catA}$. Standard deviations were calculated with the KaleidaGraph program.

[b] ND, not determined.

ing muconate cycloisomerases (*catB*) (Fig. 2A) were identified. Upstream of the *catBCA* gene cluster, the incomplete ORF1 designated *catR* is transcribed divergently and encodes a LysR type regulator with high similarity to *catR* regulators of *Pseudomonas cat* operons (97% amino acid identity to CatR of an uncultured bacterium [AB186499] and 84% identity to CatR of *Pseudomonas fluorescens* Pf-5 [NC_004129]). This therefore reflects the presence of a typical *Pseudomonas catRBCA* gene cluster in strain MT1.

RT-PCR analysis of MT1 transcripts. To confirm that the *sal* genes are transcribed during both salicylate and 5-chlorosalicylate degradation, whereas the *cat* genes are transcribed only during growth on salicylate but not on 5-chlorosalicylate, accumulation of transcripts of *salA* and *salC* and of *catA* and *catB* was measured during growth on both of these substrates as well as on acetate. Acetate was used as a noninducing negative control, since salicylate 1-hydroxylase activity, as well as catechol 1,2-dioxygenase or muconate cycloisomerizing activity, was in fact absent (<5 U/g of protein) during growth on this substrate. When the relative expression levels between the target and the reference gene (*rpsL*) were compared to those under noninducing conditions (at a ratio of 1), significantly higher levels of *salA* and *salC* transcripts were observed in salicylate-grown (400- to 800-fold) and specifically in 5-chlorosalicylate-grown cells (approximately 2,000-fold) (Fig. 3). In contrast, expression of *catA* and *catB* genes was observed at

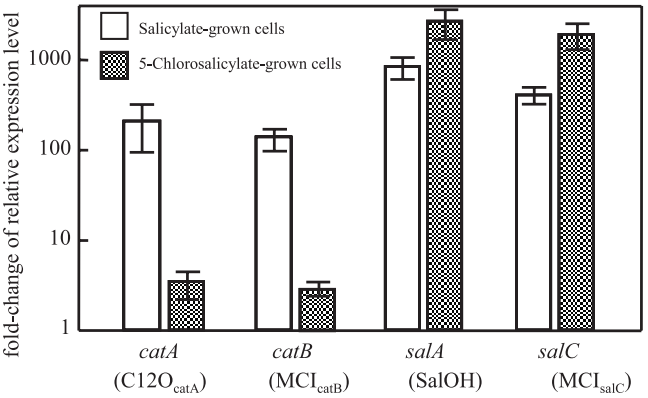

FIG. 3. Relative expression levels of catabolic genes in salicylate- and 5-chlorosalicylate-grown cells of *Pseudomonas* sp. strain MT1 as determined by quantitative RT-PCR. Values represent *n*-fold change (mean of triplicate samples) in the ratio of gene expression between the target gene and the reference gene (*rpsL*) compared to noninducing conditions (for acetate-grown cells, this ratio was set at 1).

significant levels only for salicylate-grown cells (100- to 200-fold), with only slightly elevated levels observed for cells grown with 5-chlorosalicylate (Fig. 3).

Purification and characterization of muconate cycloisomerases. Since expression analysis indicated that two distinct muconate cycloisomerases were induced during salicylate growth, we attempted to verify this by protein separation. Furthermore, since $C12O_{salD}$ was shown above to be specifically adapted for the turnover of 4-methylcatechol, the turnover of the reaction product 3-methylmuconate by MCI_{salC} was evaluated.

As previously described for 5-chlorosalicylate-grown cells (32), MCI_{salC} eluted at 0.25 ± 0.04 M NaCl during anion-exchange chromatography and at 0.06 ± 0.04 M $(NH_4)_2SO_4$ during HIC. The respective fractions not only were highly active with 3-chloromuconate and transformed it into protoanemonin (32) but also exhibited significantly higher activity with 3-methylmuconate than with muconate (activity with 0.1 mM 3-methylmuconate was approximately 20 times that obtained with 0.1 mM muconate). With salicylate extracts, a separation of two distinct activities against muconate were observed: fractions eluting at 0.6 to 0 M $(NH_4)_2SO_4$ (MCI_{salC}) were more active with 3-methylmuconate, and those eluting at 0.18 to 0.08 M $(NH_4)_2SO_4$ were more active with muconate. Further purification of the aforementioned activity and N-terminal sequencing of the prominent 42- ± 2-kDa band detected by SDS-PAGE (MLATAIESIETIIVD) verified that this was due to induction of MCI_{catB}.

Kinetic data were measured in purified enzyme fractions

Pseudomonas sp. strain KB35B NahR, DQ265742; for *P. fluorescens* Cg5 NahR, AF491310; for *P. putida* 9816-4 NahR, AF491307; for *Burkholderia gladioli* NarR, AF491314 for *P. putida* Cg1 NahR, AF491308 for *P. fluorescens* PC20 NarR, AY887963 for *Acidovorax* sp. strain JS42 NtdR, AY223676 for *Ralstonia* sp. strain U2 NagR, AF046940 for *Burkholderia* sp. strain DNT DntR, AY223677 for *P. putida* PRS2000 CatR, U12557 for *Pseudomonas* sp. strain KB35 NahG, DQ265742 for *P. putida* G7 NahG, P23262 for *P. putida* NCIB9816-4 NahG, AF491307 for *P. fluorescens* NahG, AY048764 for *P. stutzeri* AN10 NahG, AF039534 for *P. putida* KF715 NahG, Q53552 for *P. pseudoalcaligenes* KF707 SalA, DQ100350 for *Pseudomonas* sp. strain ND6 NahG (ND016), AY208917 for *P. putida* S-1 Sal, AB010714 for *Acinetobacter* sp. strain ADP1 SalA, AF150928 for *Burkholderia xenovorans* LB400 NahW, CP000272 for *Sphingomonas xenophaga* P2, AB099984 and for *P. stutzeri* AN10 NahW, AF039534.

TABLE 2. Substrate specificities of muconate cycloisomerases MCI_{catB} and MCI_{salC} from *Pseudomonas* sp. strain MT1[a]

Enzyme and substrate	Activity with 0.1 mM substrate (U/mg MCI)	K_m (μM)	k_{cat} (s^{-1})	k_{cat}/K_m (s^{-1} μM^{-1})
MCI_{catB}				
Muconate	208 ± 10	31 ± 4	186 ± 8	6.00
3-Chloromuconate	10.6 ± 1.4	99 ± 10	14.4 ± 2.2	0.15
2-Chloromuconate	<0.2	ND[b]	ND	ND
3-Methylmuconate	36.6 ± 0.9	11.1 ± 1.5	27.8 ± 1.1	2.50
2-Methylmuconate	40.2 ± 1.6	30.6 ± 5.0	36.0 ± 1.4	1.18
MCI_{salC}				
Muconate[c]	9.9 ± 1.2	1730 ± 350	125 ± 5	0.07
3-Chloromuconate[c]	35 ± 6	410 ± 75	120 ± 10	0.29
2-Chloromuconate[c]	0.09 ± 0.02	ND	ND	ND
3-Methylmuconate	239 ± 35	26.3 ± 2.3	214	8.13
2-Methylmuconate	1.0 ± 0.2	>500	ND	ND

[a] The kinetic constants were determined as described in Materials and Methods using samples where the target protein comprised 80% ± 5% (MCI_{catB}) or >99% (MCI_{salC}) of the total protein content. Activities were calculated based on the amount of target protein applied and on subunit molecular masses of 41.076 kDa for MCI_{catB} and 40.248 kDa for MCI_{salC}. Standard deviations were calculated with the KaleidaGraph program.
[b] ND, not determined.
[c] Data from reference 32.

comprising 80% ± 5% of MCI_{catB}, or >99% of MCI_{salC} (Table 2). The observed kinetic constants for MCI_{catB} were highly similar to those previously described for muconate cycloisomerase of *P. putida* PRS2000 (58): the k_{cat}/K_m specificity constants indicated that muconate was the preferred substrate, and the specificity constants with 2- and 3-methylcatechol were approximately 20 to 40% of those with muconate. The activity of MCI_{catB} with 3-chloromuconate was significantly higher than that reported for PRS2000 muconate cycloisomerase. However, it should be noted that, due to the similar spectroscopic properties of 3-chloromuconate and the reaction product protoanemonin (1), such discrepancies may reflect the unsuitability of spectrophotometric methods (such as the photometric test employed by Vollmer et al. [58]). HPLC analysis revealed that MCI_{catB} transformed 3-chloromuconate nearly quantitatively (90% ± 5%) into protoanemonin, whereas formation of *cis*-dienelactone was negligible.

By using purified MCI_{salC}, the previously analyzed kinetic data with muconate and 3-chloromuconate as substrates (32) could be confirmed. However, our new data indicated that 3-methylmuconate was preferred even over 3-chloromuconate as a substrate (Table 2). Thus, both enzymes encoded in the *sal* gene cluster ($C12O_{salD}$ and MCI_{salC}), which catalyze the turnover of catechols and muconates, were highly adapted toward 4-methylcatechol/3-methylmuconate transformation but also significantly enhanced in their turnover for 4-chlorocatechol/3-chloromuconate.

Purification of salicylate hydroxylase. Since two enzymes encoded by the *sal* gene cluster were shown to be highly adapted for transformation of methylsubstituted substrates, the kinetic properties of salicylate hydroxylase of strain MT1 were also evaluated.

The respective enzyme was purified from salicylate-grown cells by anion-exchange chromatography (eluting at 0.17 ± 0.02 M NaCl) followed by gel filtration. Fractions containing salicylate hydroxylase activity were analyzed by SDS-PAGE, and prominent bands of 48 ± 4 kDa were subjected to N-terminal sequencing. The N terminus of SalOH (NNNSSKQS LRIGXVG, where X is an unknown amino acid) was identical to that of the predicted *salA* gene product.

TABLE 3. Substrate specificities of salicylate 1-hydroxylase from *Pseudomonas* sp. strain MT1[a]

Substrate	K_m (μM)	k_{cat} (s^{-1})	k_{cat}/K_m (s^{-1} μM^{-1})
NADH	15.8 ± 2.7	5.4 ± 0.3	0.34
Salicylate	9.6 ± 1.2	4.6 ± 0.2	0.48
5-Methylsalicylate	2.4 ± 0.2	7.8 ± 0.2	3.3
4-Methylsalicylate	15.8 ± 0.9	6.4 ± 0.1	0.41
3-Methylsalicylate	12.7 ± 2.7	2.2 ± 0.2	0.17
5-Chlorosalicylate	0.6 ± 0.1	1.6 ± 0.1	2.7
4-Chlorosalicylate	2.8 ± 0.5	2.9 ± 0.1	1.0
3-Chlorosalicylate	3.8 ± 0.6	1.3 ± 0.1	0.34

[a] The kinetic constants were determined as described in Materials and Methods using samples where the target protein comprised 85% ± 5% of the total protein content. Activities were calculated based on the amount of target protein applied and on a subunit molecular mass of 50.712 kDa. Standard deviations were calculated with the KaleidaGraph program.

Kinetic data were measured in fractions comprising SalOH with a purity of at least 80% of total protein (Table 3). The highest turnover numbers were observed with 4- and 5-methylsalicylate. However, when the k_{cat}/K_m specificity constants were compared, 5-substituted salicylates were significantly preferred over salicylate as substrates by the enzyme, whereas 3-substituted salicylates were observed to be the less preferred substrates (Table 3).

Growth on 4-methyl- and 5-methylsalicylate. Since all three catalytic enzymes encoded in the salicylate cluster were highly adapted to the transformation of methylsubstituted substrates, it could be reasoned that the gene cluster has been adapted to channel 4- and 5-methylsalicylate into the *ortho* cleavage pathway. Strain MT1 was capable of growth on both 4-methyl- and 5-methylsalicylate, with growth rates of 0.49 and 0.45 h^{-1}, respectively. These rates are higher than the growth rates reported with 4-chloro- and 5-chlorosalicylate (0.05 h^{-1} and 0.16 h^{-1}, respectively) and even with salicylate (0.38 h^{-1}) (32). Analysis of cell extracts (Table 4) indicated that extradiol cleavage activity was in fact absent in MT1 grown on either of these substrates (<1 U/g protein), and in the presence of NADH, both 4- and 5-methylsalicylate were transformed quantitatively by cell extracts into 3-methylmuconolactone, as evidenced by HPLC analysis using authentic standards.

The approximately threefold higher intradiol cleavage activities with 4-methylcatechol (compared to catechol) after growth on either 4- or 5-methylsalicylate and the absence of significant activity against muconate in cell extracts (Table 4) indicated that $C12O_{salD}$ and MCI_{salC}, rather than $C12O_{catA}$ and MCI_{catB}, were induced. Separation of enzymes from 4-methylsalicylate-grown cells by HIC confirmed the absence of $C12O_{catA}$ and MCI_{catB} in the cell extract, whereas high activities of $C12O_{salD}$ and MCI_{salC} were present.

Subsequent transformation of 4-methylcatechol by partially purified $C12O_{salD}$ and MCI_{salC} resulted in quantitative formation of 4-methylmuconolactone, as evidenced by HPLC analysis using authentic standards. 4-Methylmuconolactone was

TABLE 4. Enzyme activities in cell extracts of *Pseudomonas* sp. strain MT1

Enzyme	Substrate	Sp act (U/mg of protein) after growth with:			
		Salicylate	4-Methylsalicylate	5-Methylsalicylate	Acetate
Salicylate 1-hydroxylase	Salicylate	120	85	90	<5
Catechol 2,3-dioxygenase	Catechol	<1	<1	<1	<1
Catechol 1,2-dioxygenase	Catechol	390	140	180	<5
	4-Methylcatechol	340	460	606	ND[a]
	4-Chlorocatechol	50	40	44	ND
Muconate cycloisomerase	Muconate	370	4	6	<5
	3-Methylmuconate	180	130	200	<5

[a] ND, not determined.

further transformed, by cell extracts, into 3-methylmuconolactone with activities of 80 U/g of protein. This pathway via isomerization of 4- into 3-methylmuconolactone is similar to that previously described for 4-methylcatechol transformation by JMP134 (43) and indicates the presence of a 4-methylmuconolactone 4-methylisomerase in MT1.

DISCUSSION

Catabolic gene clusters in *Pseudomonas* sp. strain MT1. *Pseudomonas* sp. strain MT1 has recently been shown to degrade 4- and 5-chlorosalicylate by a pathway that was thought to comprise a patchwork of reactions known from the classical 3-oxoadipate pathway, a *trans*-dienelactone hydrolase and a maleylacetate reductase (32). However, we show here that enzymes of the archetypal *catRBCA* gene cluster of the 3-oxoadipate pathway are not induced in *Pseudomonas* sp. strain MT1 during the growth of the strain on substituted salicylates. Rather, a new chimeric cluster comprising genes encoding a flavoprotein salicylate 1-hydroxylase and *ortho* cleavage pathway genes encoding a catechol 1,2-dioxygenase and a muconate cycloisomerase is responsible for channeling various substituted salicylates into *ortho* cleavage routes.

The genetic organization of various catechol gene clusters (*cat* genes) has been described previously (15, 16, 36, 54). The organization of the *cat* gene cluster of strain MT1 is identical to the organization characteristic for *Pseudomonas* strains and shows highest similarity to the cluster identified from an environmental metagenome library constructed from petroleum-contaminated groundwater (57). In MT1, the function of $C12O_{catA}$ and MCI_{catB} is to create, together with muconolactone isomerase, a functional catechol branch of the 3-oxoadipate pathway. This branch is induced during growth on salicylate, probably by muconate, which is generally assumed to interact with the respective CatR regulator of *catRBCA* operons (15, 35).

In MT1, two additional catechol pathway genes are located in one gene cluster together with a gene encoding salicylate 1-hydroxylase. Salicylate 1-hydroxylases are usually reported to be encoded in *sal* operons coding for the conversion of salicylate to tricarboxylic cycle intermediates through the *meta* cleavage pathway. Exceptionally, as in *Pseudomonas stutzeri* AN10 (3), a second salicylate 1-hydroxylase gene situated outside of the *sal* operon has been observed, whereas in *Acinetobacter* sp. strain ADP1 the gene encoding salicylate 1-hydroxylase is in the same transcription unit, but only with a LysR type regulator (18). The physical linkage of a salicylate 1-hydroxylase gene with genes encoding enzymes of the *ortho* cleavage pathway has, to the best of our knowledge, not been observed.

Properties of gene products of the *sal* gene cluster. Only a few proteobacterial catechol 1,2-dioxygenases have been described in detail for their catabolic properties. In all cases reported to date, catechol is the preferred substrate, as indicated by specificity constants of 30- to 100-fold that of 4-chlorocatechol (10, 52) and 6- to 40-fold that of 4-methylcatechol (10, 52, 62). $C12O_{salD}$ of MT1 is particular in this respect; its specificity constants for catechol and 4-chlorocatechol are similar, and of the substrates tested, 4-methylcatechol is the preferred substrate.

MCI_{salC} also, compared to previously described proteobacterial enzymes (53, 58), showed remarkable activities against 3-substituted muconates, with 3-chloromuconate and specifically 3-methylmuconate to be preferred over muconate as substrates. A thorough analysis of the *P. putida* PRS200-derived cycloisomerase has been performed by Vollmer et al. (58). Based on known 3-dimensional structures, variants of the cycloisomerase had been constructed by site-directed mutagenesis; an I54V (numbering according to MCI of *P. putida* PRS2000) derivative showed a significant increase in turnover of 3-chloromuconate, and 3-methylmuconate was the preferred substrate for this derivative (58). Sequence analysis revealed that MCI_{salC}, but not MCI_{catB}, harbored a valine residue at the appropriate position, in contrast to all other natural proteobacterial gene variants reported thus far. It can therefore be reasoned that this variation is at least partially responsible for the extraordinary substrate specificity of MCI_{salC}. However, compared to the I54V derivative, MCI_{salC} showed a 30-fold higher k_{cat} and a significantly lower affinity with muconate, an effect not reached by any of the site-directed mutants constructed by Vollmer et al. (58). Further investigations are thus necessary to unravel the underlying reason for MCI_{salC} substrate specificity.

In contrast to MCI_{salC} and $C12O_{salD}$, SalOH does not differ significantly in kinetic parameters from previously described enzymes. Generally, salicylate 1-hydroxylases have broad substrate specificity and can transform various monosubstituted salicylates (3, 27, 64). Unfortunately, no thorough investigation on kinetic parameters is available, and generally, only V_{max} values or k_{cat} values are given. Usually, 4- and 5-methylsalicylate are transformed at a higher rate comparable to that of salicylate, whereas 4- and 5-chlorosalicylates are transformed less effectively.

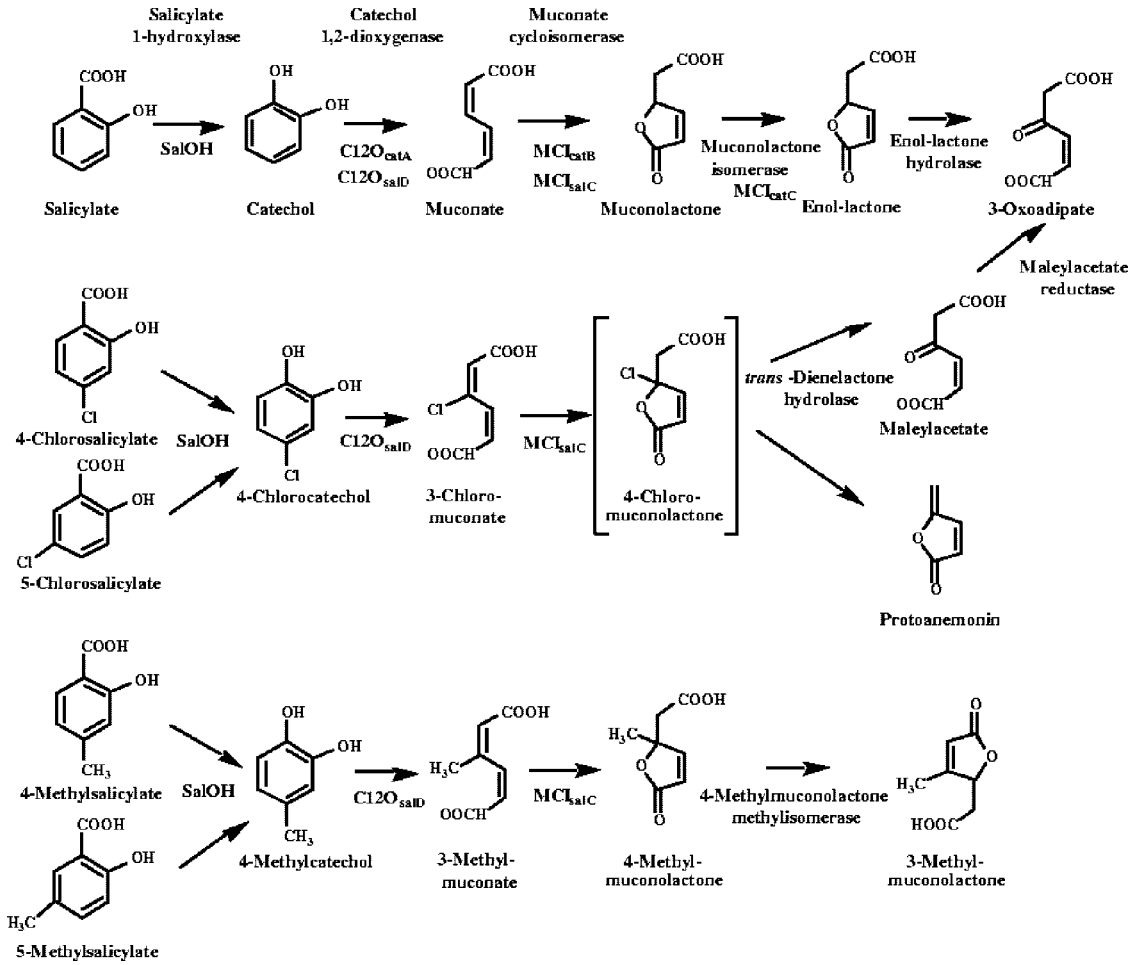

FIG. 4. Metabolism of salicylate, 4- and 5-chlorosalicylate, and 4- and 5-methylsalicylate by *Pseudomonas* sp. strain MT1. Enzyme steps common to the degradation of these substrates are given at the top, and the specific isoenzymes induced during growth on each substrate are given below the corresponding enzyme steps. Hypothetical intermediates are shown in brackets. The formation of protoanemonin from 4-chloromuconolactone is either spontaneous or catalyzed by muconate cycloisomerases.

Role of the *sal* gene cluster. In strain MT1, the function of the *sal* cluster is to effectively funnel 4- and 5-substituted salicylates into the *ortho* cleavage pathway (Fig. 4). For 4- and 5-methylsalicylate, transformation by enzymes of this cluster results in the formation of 4-methylmuconolactone (Fig. 4), a compound previously described as a dead-end product in *Pseudomonas* strains (8, 25). Transformation of this compound in *C. necator* JMP134 (39) and *R. rhodochrous* N75 (6), is catalyzed by a 4-methylmuconolactone methylisomerase transforming 4- into 3-methylmuconolactone (7, 43). This transformation allows a further degradation by muconolactone isomerases, in analogy to the 3-oxoadipate pathway, by abstracting a proton from the C-4 carbon (45). In fact, an operon comprising both a gene encoding 4-methylmuconolactone methylisomerase and a gene encoding methylmuconolactone isomerase has been identified in JMP 134 (13), and homologous genes have been identified in *Cupriavidus necator* H16 (PHG6385, NC_005241). Clearly, MT1 uses a similar pathway for degradation of 4-methylmuconolactone by initially isomerizing it into 3-methylmuconolactone. However, in contrast to the situation with *C. necator*, which also harbors catechol *meta* cleavage pathways (21, 22) and is reported to degrade methylaromatics by both intra- and extradiol cleavage (40, 41), MT1 metabolizes methylsalicylates exclusively via the *ortho* cleavage pathway (Fig. 4). A prerequisite for funneling methylaromatics into *ortho* cleavage pathways is the induction of both a catechol 1,2-dioxygenase and a muconate cycloisomerase during growth on methylaromatics. At least for *Pseudomonas* MT1, the *cat* gene cluster is not induced during growth on 4- or 5-methylsalicylate (or on 5-chlorosalicylate). Considering that CatR regulators are usually responsive to muconate (29, 35), it can be suggested that CatR of MT1 is not responsive, or at least is only poorly responsive, to 3-methylmuconate. Unfortunately, no information is available on detailed effector specificities of CatR proteins.

A similar strain capable of degrading methylbenzoate exclusively via the *ortho* cleavage pathway was previously obtained only after extensive genetic engineering (50). The goal of that approach had been to obtain a strain capable of simultaneously degrading both methyl- and chloroaromatics via *ortho* cleavage routes. Clearly, strain MT1 harbors that capability naturally. For the degradation of chlorosalicylates, strain MT1 has been

reported to recruit a *trans*-dienelactone hydrolase capable of hydrolyzing 4-chloromuconolactone, the unstable intermediate of 3-chloromuconate transformation, thereby preventing the formation of protoanemonin (32). Identification and localization of the respective gene, which, together with the *sal* gene cluster and a gene encoding maleylacetate reductase, form a functional pathway for chlorosalicylate degradation, are currently in progress.

ACKNOWLEDGMENTS

The work was supported by the DFG-European Graduate College 653.

We thank Rita Getzlaff (GBF) for N-terminal protein amino acid sequencing and Agnes Waliczek for support in preparation of gene libraries. We gratefully acknowledge Andrew Oxley, Hannes Nahrstedt, and Howard Junca for inspiring discussions.

REFERENCES

1. **Blasco, R., R.-M. Wittich, M. Mallavarapu, K. N. Timmis, and D. H. Pieper.** 1995. From xenobiotic to antibiotic. Formation of protoanemonin from 4-chlorocatechol by enzymes of the 3-oxoadipate pathway. J. Biol. Chem. **270:**29229–29235.
2. **Bosch, R., E. Garcia-Valdes, and E. R. B. Moore.** 1999. Genetic characterization and evolutionary implications of a chromosomally encoded naphthalene-degradation upper pathway from *Pseudomonas stutzeri* AN10. Gene **236:**149–157.
3. **Bosch, R., E. R. B. Moore, E. Garcia Valdes, and D. H. Pieper.** 1999. NahW, a novel, inducible salicylate hydroxylase involved in mineralization of naphthalene by *Pseudomonas stutzeri* AN10. J. Bacteriol. **181:**2315–2322.
4. **Bradford, M. M.** 1976. A rapid and sensitive method for the quantitation of protein utilizing the principle of protein-dye binding. Anal. Biochem. **72:** 248–254.
5. **Briganti, F., E. Pessione, C. Giunta, and A. Scozzafava.** 1997. Purification, biochemical properties and substrate specificity of a catechol 1,2-dioxygenase from a phenol degrading *Acinetobacter radioresistens*. FEBS Lett. **416:** 61–64.
6. **Bruce, N. C., and R. B. Cain.** 1988. β-Methylmuconolactone, a key intermediate in the dissimilation of methylaromatic compounds by a modified 3-oxoadipate pathway evolved in nocardioform actinomycetes. FEMS Microbiol. Lett. **50:**233–239.
7. **Bruce, N. C., R. B. Cain, D. H. Pieper, and K.-H. Engesser.** 1989. Purification and characterization of 4-methylmuconolactone methyl-isomerase, a novel enzyme of the modified 3-oxoadipate pathway in nocardioform actinomycetes. Biochem. J. **262:**303–312.
8. **Catelani, D., A. Fiecchi, and E. Galli.** 1971. (+)-γ-Carboxymethyl-γ-methyl-Δ^{α}-butenolide. A 1,2-ring-fission product of 4-methylcatechol by *Pseudomonas desmolyticum*. Biochem. J. **121:**89–92.
9. **Dennis, J., and G. Zylstra.** 2004. Complete sequence and genetic organization of pDTG1, the 83 kilobase naphthalene degradation plasmid from *Pseudomonas putida* strain NCIB 9816-4. J. Mol. Biol. **341:**753–768.
10. **Dorn, E., and H.-J. Knackmuss.** 1978. Chemical structure and biodegradability of halogenated aromatic compounds. Substituent effects on 1,2-dioxygenation of catechol. Biochem. J. **174:**85–94.
11. **Dorn, E., and H.-J. Knackmuss.** 1978. Chemical structure and biodegradability of halogenated aromatic compounds. Two catechol 1,2-dioxygenases from a 3-chlorobenzoate-grown pseudomonad. Biochem. J. **174:**73–84.
12. **Dumas, J., C. van Delden, K. Perron, and T. Koehler.** 2006. Analysis of antibiotic resistance gene expression in *Pseudomonas aeruginosa* by quantitative real-time-PCR. FEMS Microbiol. Lett. **254:**217–225.
13. **Erb, R., K. Timmis, and D. Pieper.** 1998. Characterization of a gene cluster from *Ralstonia eutropha* JMP134 encoding metabolism of 4-methylmuconolactone. Gene **206:**53–62.
14. **Galvao, T., and V. de Lorenzo.** 2006. Transcriptional regulators à la carte: engineering of new effector specificities in bacterial regulatory proteins. Curr. Opin. Biotechnol. **17:**34–42.
15. **Harwood, C. S., and R. E. Parales.** 1996. The beta-ketoadipate pathway and the biology of self-identity. Annu. Rev. Microbiol. **50:**553–590.
16. **Jimenez, J. I., B. Minambres, J. L. Garcia, and E. Diaz.** 2002. Genomic analysis of the aromatic catabolic pathways from *Pseudomonas putida* KT2440. Environ. Microbiol. **4:**824–841.
17. **Jimenez, J. I., B. Minambres, J. L. Garcia, and E. Diaz.** 2004. Genomic insights in the metabolism of aromatic compounds in *Pseudomonas*, p. 425–462. *In* J. L. Ramos (ed.), The Pseudomonads, vol. 3. Biosynthesis of macromolecules and molecular metabolism. Kluwer Academic/Plenum Publishers, New York, NY.
18. **Jones, R. M., V. Pagmantidis, and P. A. Williams.** 2000. *sal* genes determining the catabolism of salicylate esters are part of a supraoperonic cluster of catabolic genes in *Acinetobacter* sp. strain ADP1. J. Bacteriol. **182:**2018–2025.
19. **Junca, H., and D. Pieper.** 2004. Functional gene diversity analysis in BTEX contaminated soils by means of PCR-SSCP DNA fingerprinting: comparative diversity assessment against bacterial isolates and PCR-DNA clone libraries. Environ. Microbiol. **6:**95–110.
20. **Junca, H., I. Plumeier, H. Hecht, and D. Pieper.** 2004. Difference in kinetic behaviour of catechol 2,3-dioxygenase variants from a polluted environment. Microbiology **150:**4181–4187.
21. **Kabisch, M., and P. Fortnagel.** 1990. Nucleotide sequence of metapyrocatechase I (catechol 2,3-oxygenase I) gene *mpcI* from *Alcaligenes eutrophus* JMP222. Nucleic Acids Res. **18:**3405–3406.
22. **Kabisch, M., and P. Fortnagel.** 1990. Nucleotide sequence of the metapyrocatechase II (catechol 2,3-oxygenase II) gene *mpcII* from *Alcaligenes eutrophus* JMP 222. Nucleic Acids Res. **18:**5543.
23. **Kaschabek, S. R., and W. Reineke.** 1992. Maleylacetate reductase of *Pseudomonas* sp. strain B13: dechlorination of chloromaleylacetates, metabolites in the degradation of chloroaromatic compounds. Arch. Microbiol. **158:**412–417.
24. **Kim, S. I., S. H. Leem, J. S. Choi, Y. H. Chung, S. Kim, Y. M. Park, Y. K. Park, Y. N. Lee, and K. S. Ha.** 1997. Cloning and characterization of two *catA* genes in *Acinetobacter lwoffii* K24. J. Bacteriol. **179:**5226–5231.
25. **Knackmuss, H.-J., M. Hellwig, H. Lackner, and W. Otting.** 1976. Cometabolism of 3-methylbenzoate and methylcatechols by a 3-chlorobenzoate utilizing *Pseudomonas*: accumulation of (+)-2,5-dihydro-4-methyl- and (+)-2,5-dihydro-2-methyl-5-oxo-furan-2-acetic acid. Eur. J. Appl. Microbiol. **2:**267–276.
26. **Laemmli, U. K.** 1970. Cleavage of structural proteins during the assembly of the head of bacteriophage T4. Nature **227:**680–685.
27. **Lamanda, A., A. Zahn, D. Roder, and H. Langen.** 2004. Improved Ruthenium II tris (bathophenantroline disulfonate) staining and destaining protocol for a better signal-to-background ratio and improved baseline resolution. Proteomics **4:**599–608.
28. **Li, W., J. D. Shi, X. G. Wang, Y. N. Han, W. Tong, L. Ma, B. Liu, and B. L. Cai.** 2004. Complete nucleotide sequence and organization of the naphthalene catabolic plasmid pND6-1 from *Pseudomonas* sp. strain ND6. Gene **336:**231–240.
29. **McFall, S. M., S. A. Chugani, and A. M. Chakrabarty.** 1998. Transcriptional activation of the catechol and chlorocatechol operons: variations on a theme. Gene **223:**257–267.
30. **Murakami, S., A. Takashima, J. Takemoto, S. Takenaka, R. Shinke, and K. Aoki.** 1999. Cloning and sequence analysis of two catechol-degrading gene clusters from the aniline-assimilating bacterium *Frateuria* species ANA-18. Gene **226:**189–198.
31. **Nakai, C., T. Nakazawa, and M. Nozaki.** 1988. Purification and properties of catechol 1,2-dioxygenase (pyrocatechase) from *Pseudomonas putida* mt-2 in comparison with that from *Pseudomonas arvilla* C-1. Arch. Biochem. Biophys. **267:**701–713.
32. **Nikodem, P., V. Hecht, M. Schlömann, and D. H. Pieper.** 2003. New bacterial pathway for 4- and 5-chlorosalicylate degradation via 4-chlorocatechol and maleylacetate in *Pseudomonas* sp. strain MT1. J. Bacteriol. **185:**6790–6800.
33. **Nojiri, H., K. Maeda, H. Sekiguchi, M. Urata, M. Shintani, T. Yoshida, H. Habe, and T. Omori.** 2002. Organization and transcriptional characterization of catechol degradation genes involved in carbazole degradation by *Pseudomonas resinovorans* strain CA10. Biosci. Biotechnol. Biochem. **66:**897–901.
34. **Page, R.** 1996. TREEVIEW: an application to display phylogenetic trees on personal computers. Comput. Appl. Biosci. **12:**357–358.
35. **Parsek, M. R., D. L. Shinabarger, R. K. Rothmel, and A. M. Chakrabarty.** 1992. Roles of CatR and *cis*, *cis*-muconate in activation of the *catBC* operon, which is involved in benzoate degradation in *Pseudomonas putida*. J. Bacteriol. **174:**7798–7806.
36. **Paulsen, I. T., C. M. Press, J. Ravel, D. Y. Kobayashi, G. S. Myers, D. V. Mavrodi, R. T. DeBoy, R. Seshadri, Q. Ren, R. Madupu, R. J. Dodson, A. S. Durkin, L. M. Brinkac, S. C. Daugherty, S. A. Sullivan, M. J. Rosovitz, M. L. Gwinn, L. Zhou, D. J. Schneider, S. W. Cartinhour, W. C. Nelson, J. Weidman, K. Watkins, K. Tran, H. Khouri, E. A. Pierson, L. S. Pierson III, L. S. Thomashow, and J. E. Loper.** 2005. Complete genome sequence of the plant commensal *Pseudomonas fluorescens* Pf-5. Nat. Biotechnol. **23:**873–878.
37. **Pfaffl, M. W., G. W. Horgan, and L. Dempfle.** 2002. Relative expression software tool (REST) for group-wise comparison and statistical analysis of relative expression results in real-time PCR. Nucleic Acids Res. **30:**e36.
38. **Pieper, D., and W. Reineke.** 2004. Degradation of chloroaromatics by Pseudomona(d)s, p. 509–574. *In* J. L. Ramos (ed.), The Pseudomonads, vol. 3. Biosynthesis of macromolecules and molecular metabolism. Kluwer Academic/Plenum Publishers, New York, NY.
39. **Pieper, D. H., K.-H. Engesser, R. H. Don, K. N. Timmis, and H.-J. Knackmuss.** 1985. Modified *ortho*-cleavage pathway in *Alcaligenes eutrophus* JMP134 for the degradation of 4-methylcatechol. FEMS Microbiol. Lett. **29:**63–67.
40. **Pieper, D. H., K.-H. Engesser, and H.-J. Knackmuss.** 1989. Regulation of catabolic pathways of phenoxyacetic acids and phenols in *Alcaligenes eutrophus* JMP 134. Arch. Microbiol. **151:**365–371.

41. **Pieper, D. H., W. Reineke, K.-H. Engesser, and H.-J. Knackmuss.** 1988. Metabolism of 2,4-dichlorophenoxyacetic acid, 4-chloro-2-methylphenoxyacetic acid and 2-methylphenoxyacetic acid by *Alcaligenes eutrophus* JMP 134. Arch. Microbiol. **150:**95–102.
42. **Pieper, D. H., K. Stadler-Fritzsche, K.-H. Engesser, and H.-J. Knackmuss.** 1993. Metabolism of 2-chloro-4-methylphenoxyacetate by *Alcaligenes eutrophus* JMP 134. Arch. Microbiol. **160:**169–178.
43. **Pieper, D. H., K. Stadler-Fritzsche, H.-J. Knackmuss, K. H. Engesser, N. C. Bruce, and R. B. Cain.** 1990. Purification and characterization of 4-methylmuconolactone methylisomerase, a novel enzyme of the modified 3-oxoadipate pathway in the Gram-negative bacterium *Alcaligenes eutrophus* JMP 134. Biochem. J. **271:**529–534.
44. **Potrawfke, T., J. Armengaud, and R. M. Wittich.** 2001. Chlorocatechols at positions 4 and 5 are substrates of the broad-spectrum chlorocatechol 1,2-dioxygenase of *Pseudomonas chlororaphis* RW71. J. Bacteriol. **183:**997–1011.
45. **Prucha, M., A. Peterseim, and D. H. Pieper.** 1997. Evidence for an isomeric muconolactone isomerase involved in the metabolism of 4-methylmuconolactone by *Alcaligenes eutrophus* JMP134. Arch. Microbiol. **168:**33–38.
46. **Prucha, M., V. Wray, and D. H. Pieper.** 1996. Metabolism of 5-chlorosubstituted muconolactones. Eur. J. Biochem. **237:**357–366.
47. **Reams, A. B., and E. L. Neidle.** 2003. Genome plasticity in *Acinetobacter*: new degradative capabilities acquired by the spontaneous amplification of large chromosomal segments. Mol. Microbiol. **47:**1291–1304.
48. **Reineke, W.** 1998. Development of hybrid strains for the mineralization of chloroaromatics by patchwork assembly. Annu. Rev. Microbiol. **52:**287–331.
49. **Reineke, W., and H.-J. Knackmuss.** 1988. Microbial degradation of haloaromatics. Annu. Rev. Microbiol. **42:**263–287.
50. **Rojo, F., D. H. Pieper, K. H. Engesser, H. J. Knackmuss, and K. N. Timmis.** 1987. Assemblage of *ortho* cleavage route for simultaneous degradation of chloro- and methylaromatics. Science **238:**1395–1398.
51. **Sambrook, J., E. F. Fritsch, and T. Maniatis.** 1989. Molecular cloning: a laboratory manual, 2nd ed. Cold Spring Harbor Laboratory Press, Cold Spring Harbor, NY.
52. **Sauret-Ignazi, G., J. Gagnon, C. Beguin, M. Barrelle, Y. Markowicz, J. Pelmont, and A. Toussaint.** 1996. Characterisation of a chromosomally encoded catechol 1,2-dioxygenase (EC 1.13.11.1) from *Alcaligenes eutrophus* CH34. Arch. Microbiol. **166:**42–50.
53. **Schmidt, E., and H.-J. Knackmuss.** 1980. Chemical structure and biodegradability of halogenated aromatic compounds. Conversion of chlorinated muconic acids into maleoylacetic acid. Biochem. J. **192:**339–347.
54. **Stover, C. K., X. Q. Pham, A. L. Erwin, S. D. Mizoguchi, P. Warrener, M. J. Hickey, F. S. L. Brinkman, W. O. Hufnagle, D. J. Kowalik, M. Lagrou, R. L. Garber, L. Goltry, E. Tolentino, S. Westbrock-Wadman, Y. Yuan, L. L. Brody, S. N. Coulter, K. R. Folger, A. Kas, K. Larbig, R. Lim, K. Smith, D. Spencer, G. K. S. Wong, Z. Wu, I. T. Paulsen, J. Reizer, M. H. Saier, R. E. W. Hancock, S. Lory, and M. V. Olson.** 2000. Complete genome sequence of *Pseudomonas aeruginosa* PAO1, an opportunistic pathogen. Nature **406:**959–964.
55. **Suzuki, K., A. Ichimura, N. Ogawa, A. Hasebe, and K. Miyashita.** 2002. Differential expression of two catechol 1,2-dioxygenases in *Burkholderia* sp. strain TH2. J. Bacteriol. **184:**5714–5722.
56. **Thompson, J. D., T. J. Gibson, F. Plewniak, F. Jeanmougin, and D. G. Higgins.** 1997. The CLUSTAL_X windows interface: flexible strategies for multiple sequence alignment aided by quality analysis tools. Nucleic Acids Res. **25:**4876–4882.
57. **Uchiyama, T., T. Abe, T. Ikemura, and K. Watanabe.** 2005. Substrate-induced gene-expression screening of environmental metagenome libraries for isolation of catabolic genes. Nat. Biotechnol. **23:**88–93.
58. **Vollmer, M. D., H. Hoier, H. J. Hecht, U. Schell, J. Groning, A. Goldman, and M. Schlömann.** 1998. Substrate specificity of and product formation by muconate cycloisomerases: an analysis of wild-type enzymes and engineered variants. Appl. Environ. Microbiol. **64:**3290–3299.
59. **Vollmer, M. D., and M. Schlömann.** 1995. Conversion of 2-chloro-*cis*, *cis*-muconate and its metabolites 2-chloro- and 5-chloromuconolactone by chloromuconate cycloisomerase of pJP4 and pAC27. J. Bacteriol. **177:**2938–2941.
60. **Vollmer, M. K., P. Fischer, H.-J. Knackmuss, and M. Schlömann.** 1994. Inability of muconate cycloisomerases to cause dehalogenation during conversion of 2-chloro-*cis*, *cis*-muconate. J. Bacteriol. **176:**4366–4375.
61. **Wallis, M., and S. Chapman.** 1990. Isolation and partial characterization of an extradiol non-haem iron dioxygenase which preferentially cleaves 3-methylcatechol. Biochem. J. **266:**605–609.
62. **Wang, C. L., S. Takenaka, S. Murakami, and K. Aoki.** 2001. Production of catechol from benzoate by the wild strain *Ralstonia* species Ba-0323 and characterization of its catechol 1,2-dioxygenase. Biosci. Biotechnol. Biochem. **65:**1957–1964.
63. **Yen, K.-M., and C. M. Serdar.** 1988. Genetics of naphthalene catabolism in *Pseudomonas*. Crit. Rev. Microbiol. **15:**247–268.
64. **Zhao, H., D. Chen, Y. Li, and B. Cai.** 2005. Overexpression, purification and characterization of a new salicylate hydroxylase from naphthalene-degrading *Pseudomonas* sp. strain ND6. Microbiol. Res. **160:**307–313.